Complex Fluid Flows and Its Environmental Applications

University of Lagos, Nigeria

$6^{th} - 11^{th}$ June 2016

Dr. Najmeh Foroozani

The Abdus Salam International Centre for Theoretical Physics (ICTP), Trieste Italy

nforooza@ictp.it

www.ictp.it

The Abdus Salam International Centre for Theoretical Physics

Computational Fluid Dynamics (CFD)

Computational fluid dynamics, usually abbreviated as CFD, is a branch of fluid mechanics that uses numerical analysis and algorithms to solve and analyze problems that involve fluid flows. Computational Fluid Dynamics (CFD) is the science of predicting fluid flow, heat and mass transfer, chemical reactions, and related phenomena. To predict these phenomena, CFD solves equations for conservation of mass, momentum, energy etc.. CFD is used in all stages of the engineering process:

• Conceptual studies of new designs

• Detailed product development

• Optimization

• Troubleshooting

• Redesign CFD analysis complements testing and experimentation by reducing total effort and cost required for experimentation and data acquisition.

Previously Available Methods Historically there were two broad methodologies for solving fluid flow problems:

1. Analytical Fluid Dynamics (AFD); The exact solutions of fluid flow problems were found by applying first principles of fluid dynamics along with mathematical modelling of the entire fluid domain by various mathematical techniques. But even a little increase in fluid model the mathematical exponentially increased. Further it is practically impossible to mathematically model complicated fluid flow situations. Weakness: Cannot be independently verified and very difficult for complex flow.

2. Experimental Fluid Dynamics (EFD); Previously Available Methods Experimental Fluid Dynamics (EFD) : The flow problem is solved by making a model of the domain and the measurable flow properties are measured using various measurement techniques(such as hot wire anemometry, Acoustics Doppler Current Profiler) and then other properties can be calculated using imperial relationships. Moreover, Experimental Fluid Dynamics was used to verify the results obtained from Analytical Fluid Dynamics. Weakness: loss of (significant/insignificant) similitude in case of extremely large and small domains and error in measurements.

3. Computational Fluid Dynamics (CFD); Birth of CFD with the advance of computational capabilities and numerical techniques in 1950s various alternate methods to solve fluid flow problems were found under the common name CFD. This involved: Constructing a fluid domain to be analyzed. Applying Suitable Boundary Conditions. Breaking the domain into finite small elements using discretization methods. Generating differential equations for each of the generated element. Converting of each of the differential equation into a linear equation using numerical techniques. Using the Computational Capabilities to solve these equations in an iterative fashion. Bringing together all the elements properties and use suitable interpolation for the final results.

Is CFD an Independent Technique?

Although it seems that everything we need to analyze a fluid domain is already in there. But it is not the case. It is just a simulation and the authenticity of the simulation cannot be verified unless it is compared with the real world. Experimental Fluid Dynamics is used to test the validity of a CFD simulation and is more or less an approval that the CFD model is correct and can further be applied to similar situations without even getting verified. CFD is indeed a very powerful TOOL if used wisely.

1. It can be used to study fluid flows in visually obstructed situations (ex. Flows in nuclear reactor, combustion chamber etc.)
2. It can be used to short list experiments to find the best options that can be the solution.
3. To help get hands on more comprehensive results in the fluid domain that couldn’t have been possible with experiments alone

Turbulence Models

A turbulence model is a computational procedure to close the system of mean flow equations. For most engineering applications it is unnecessary to resolve the details of the turbulent fluctuations. Turbulence models allow the calculation of the mean flow without first calculating the full time-dependent flow field. We only need to know how turbulence affected the mean

flow. In particular, we need expressions for the Reynolds stresses. For a turbulence model to be useful it.

1. must have wide applicability
2. be accurate
3. simple
4. economical to run

Based on Reynolds Averaged Navier-Stokes (RANS) equations (time averaged):

1. Zero equation model: mixing length model
2. One equation model: Spalart-Almaras
3. Two equation models: k- ε style models (standard, RNG, realizable), k- ω model
4. Seven equation model: Reynolds stress model. The number of equations denotes the number of additional PDEs that are being solved.

To solve the governing equations of motions (NS equations) approximately, we are happy to just find the quantities at set of points. Hence we discretize the domain into a grid points (that's the trick!!)

Discretization Methods; In order to solve the governing equations of the fluid motion, first their numerical analogue must be generated. This is done by a process referred to as discretization. In the discretization process, each term within the partial differential equation describing the flow is written in such a manner that the computer can be programmed to calculate. There are various techniques for numerical discretization. Here we will introduce three of the most commonly used techniques, namely: (1) The finite difference method (2) The finite element method (3) The finite volume method

The Finite Volume Method; The finite volume method is currently the most popular method in CFD. Generally, the finite volume method is a special case of finite element. A typical finite volume, or cell, is shown. In this figure the centroid of the volume, point P, is the reference point at which we want to discretize the partial differential equation. This method is also referred to as the Cell Centered (CC) Method, where the flow variables are allocated at the center of the computational cell. The CC variable arrangement is the most popular, since it leads to considerably simpler implementations than other arrangements. On the other hand, the CC arrangement is more susceptible to truncation errors, when the mesh departs from uniform rectangles. Traditionally the finite volume methods have used regular grids for the efficiency of the computations. However, recently, irregular grids have become more popular for simulating flows in complex geometries. Obviously, the computational effort is more when irregular grids are used, since the algorithm should use a table to lookup the geometrical relationships between the volumes or element faces.

CFD codes are structured around the numerical algorithms that can tackle fluid flow problems. In order to provide easy access to their solving power all commercial CFD packages include sophisticated user interfaces to input problem parameters and to examine the results. Hence all codes contain three main elements: 1. Pre-processor 2. Solver 3. Post-processor

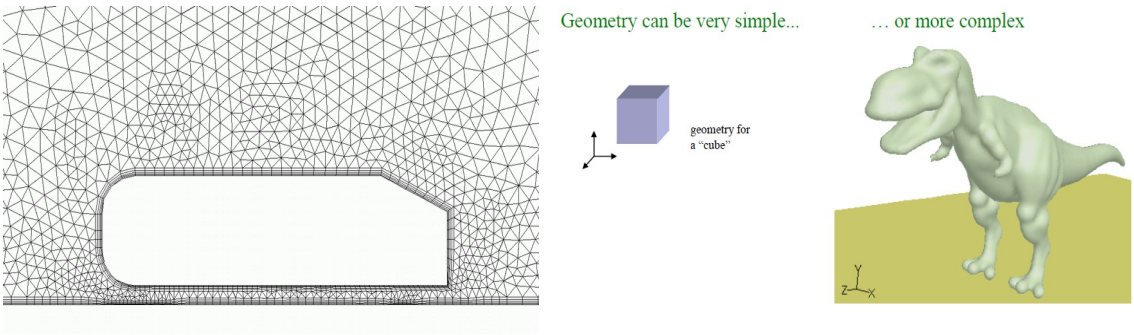

Design and create the mesh

Meshing in computational solutions of partial differential equations, meshing is a discrete representation of the geometry that is involved in the problem. Essentially, it partitions space into elements (or cells or zones) over which the equations can be approximated. Zone boundaries can be free to create computationally best shaped zones, or they can be fixed to represent internal or external boundaries within a model. The mesh quality can be conclusively determined based on the following factors.

• Rate of convergence The greater the rate of convergence, the better the mesh quality. It means that the correct solution has been achieved faster. An inferior mesh quality may leave out certain important phenomena such as the boundary layer that occurs in fluid flow. In this case the solution may not converge or the rate of convergence will be impaired.

• Solution accuracy A better mesh; quality provides a more accurate solution. For example, one can refine the mesh at certain areas of the geometry where the gradients are high, thus increasing the fidelity of solutions in the region. Also, this means that if a mesh is not sufficiently refined then the accuracy of the solution is more limited. Thus, mesh quality is dictated by the required accuracy.

• CPU time required CPU time is a necessary yet undesirable factor. For a highly refined mesh, where the number of cells per unit area is maximum, the CPU time required will be relatively large. Time will generally be proportional to the number of elements.

Meshing Common cell shapes:

1)Two dimensional; There are two types of two-dimensional cell shapes that are commonly used. These are the triangle and the quadrilateral. Computationally poor elements will have sharp internal angles or short edges or both.

• Triangle This cell shape consists of 3 sides and is one of the simplest types of mesh. A triangular surface mesh is always quick and easy to create. It is most common in unstructured grids.

• Quadrilateral This cell shape is a basic 4 sided one as shown in the figure. It is most common in structured grids. Quadrilateral elements are usually excluded from being or becoming concave.

2)Three dimensional; The basic 3-dimensional element are the tetrahedron, quadrilateral pyramid, triangular prism, and hexahedron. They all have triangular and quadrilateral faces. Extruded 2-dimensional models may be represented entirely by prisms and hexahedra as extruded triangles and quadrilaterals. In general, quadrilateral faces in 3-dimensions may not be perfectly planar. A nonplanar quadrilateral face can be considered a thin tetrahedral volume that is shared by two neighboring elements. Tetrahedron A tetrahedron has 4 vertices, 6 edges, and is bounded by 4 triangular faces. In most cases a tetrahedral volume mesh can be generated automatically. Pyramid A quadrilateral-based pyramid has 5 vertices, 8 edges, bounded by 4 triangular and 1 quadrilateral face. These are effectively used as transition elements between square and triangular faced elements and other in hybrid meshes and grids. Triangular prism A triangular prism has 6 vertices, 9 edges, bounded by 2 triangular and 3 quadrilateral faces. The advantage with this type of layer is that it resolves boundary layer efficiently. Hexahedron A hexahedron, a topological cube, has 8 vertices, 12 edges, bounded by 6 quadrilateral faces. It is also called a hex or a brick. For the same cell amount, the accuracy of solutions in hexahedral meshes is the highest. The pyramid and triangular prism zones can be considered computationally as degenerate hexahedrons, where some edges have been reduced to zero. Other degenerate forms of a hexahedron may also be represented.

Structured grids; Structured grids are identified by regular connectivity. The possible element choices are quadrilateral in 2D and hexahedra in 3D. This model is highly space efficient, i.e. since the neighborhood relationships are defined by storage arrangement. Some other advantages of structured grid over unstructured are better convergence and higher resolution.

Unstructured grids; An unstructured grid is identified by irregular connectivity. It cannot easily be expressed as a two-dimensional or three-dimensional array in computer memory. This allows for any possible element that a solver might be able to use. Compared to structured meshes, this model can be highly space inefficient since it calls for explicit storage of neighborhood relationships. These grids typically employ triangles in 2D and tetrahedra in 3D. • Hybrid/multizone grids A hybrid grid contains a mixture of structured portions and unstructured portions. It integrates the structured meshes and the unstructured meshes in an efficient manner. Those parts of the geometry that are regular can have structured grids and those that are complex can have unstructured grids. These grids can be non- conformal which means that grid lines don’t need to match at block boundaries.

Solver

There are three distinct streams of numerical solution techniques: finite difference, finite element and spectral methods. We shall be solely concerned with the finite volume method, a special finite difference formulation that is central to the most well-established CFD codes: CFX/ANSYS, FLUENT, PHOENICS and STAR-CD. In outline the numerical algorithm consists of the following steps:

• Integration of the governing equations of fluid flow over all the (finite) control volumes of the domain

• Discretization – conversion of the resulting integral equations into a system of algebraic equations

• Solution of the algebraic equations by an iterative method

The first step, the control volume integration, distinguishes the finite volume method from all other CFD techniques. The resulting statements express the (exact) conservation of relevant properties for each finite size cell. This clear relationship between the numerical algorithm and the underlying physical conservation principle forms one of the main attractions of the finite volume method and makes its concepts much more simple to understand by engineers than the finite element and spectral methods. The conservation of a general flow variable φ, e.g. a velocity component or enthalpy, within a finite control volume can be expressed as a balance between the various processes tending to increase or decrease it. In words we have: CFD codes contain discretization techniques suitable for the treatment of the key transport phenomena, convection (transport due to fluid flow) and diffusion (transport due to variations of φ from point to point) as well as for the source terms (associated with the creation or destruction of φ) and the rate of change with respect to time. The underlying physical phenomena are complex and non-linear so an iterative solution approach is required.

> Pre-processing consists of the input of a flow problem to a CFD program by means of an operator-friendly interface and the subsequent transformation of this input into a form suitable for use by the solver. The user activities at the pre-processing stage involve: • Definition of the geometry of the region of interest: the computational domain • Grid generation – the sub-division of the domain into a number of smaller, non- overlapping sub-domains: a grid (or mesh) of cells (or control volumes or elements) • Selection of the physical and chemical phenomena that need to be modelled • Definition of fluid properties • Specification of appropriate boundary conditions at cells which coincide with or touch the domain boundary

As in pre-processing, a huge amount of development work has recently taken place in the post-processing field. Due to the increased popularity of engineering workstations, many of which have outstanding graphics capabilities, the leading CFD packages are now equipped with versatile data visualization tools. These include:

• Domain geometry and grid display

• Vector plots

• Line and shaded contour plots

• 2D and 3D surface plots

• Particle tracking

• View manipulation (translation, rotation, scaling

Numerical models

Turbulence is that state of fluid motion which is characterized by apparently random and chaotic three-dimensional vorticity. When turbulence is present, it usually dominates all other flow phenomena and results in increased energy dissipation, mixing, heat transfer, and drag. If there is no three-dimensional vorticity, there is no real turbulence. The reasons for this will become clear later; but briefly, it is ability to generate new vorticity from old vorticity that is essential to turbulence. And only in a three-dimensional flow is the necessary stretching and turning of vorticity by the flow itself possible.

For a long time, scientists were not really sure in which sense turbulence is “random”, but they were pretty sure it was. Like anyone who is trained in physics, we believe the flows we see around us must be the solution to some set of equations which govern. (This is after all what mechanics is about — writing equations to describe and predict the world around us.) But because of the nature of the turbulence, it wasn’t clear whether the equations themselves had some hidden randomness, or just the solutions. And if the latter, was it something the equations did to them, or a consequence of the initial conditions?

All of this began to come into focus as we learned about the behavior of strongly non-linear dynamical systems in the past few decades. Even simple nonlinear equations with deterministic solutions and prescribed initial conditions were found to exhibit chaotic and apparently random behavior. In fact, the whole new field of chaos was born in the 1980’s, complete with its new language of strange attractors, fractals, and Lyapunov exponents. Such studies now play a major role in analyzing dynamical systems and control, and in engineering practice as well.

COMPLEXITY OF TURBULENCE MODEL

Complexity of different turbulence models may vary strongly depending on the details one wants to observe and investigate by carrying out such numerical simulations. Complexity is due to the nature of Navier-Stokes equation (N-S equation). N-S equation is inherently nonlinear, time-dependent, three-dimensional PDE.

Turbulence could be thought of as instability of laminar flow that occurs at high Reynolds number (Re). Such instabilities origin form interactions between non-linear inertial terms and viscous terms in N-S equation. These interactions are rotational, fully time-dependent and fully three-dimensional. Rotational and three-dimensional interactions are mutually connected via vortex stretching. Vortex stretching is not possible in two dimensional space. That is also why no satisfactory two-dimensional approximations for turbulent phenomena are available.

Furthermore, turbulence is thought of as random process in time. Therefore, no deterministic approach is possible. Certain properties could be learned about turbulence using statistical methods. These introduce certain correlation functions among flow variables. However, it is impossible to determine these correlations in advance. Another important feature of a turbulent flow is that vortex structures move along the flow. Their lifetime is usually very long. Hence certain turbulent quantities cannot be specified as local. This simply means that upstream history of the flow is also of great importance.

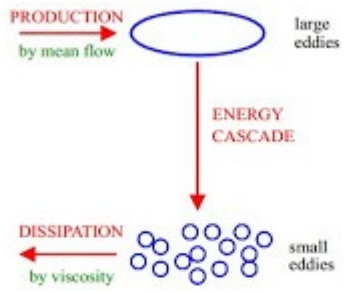

TURBULENCE PRODUCTION AND DISSIPATION

Turbulence is initially generated by instabilities in the flow caused by mean velocity gradients. These eddies in their turn breed new instabilities and hence smaller eddies. The process continues until the eddies become sufficiently small (and fluctuating velocity gradients sufficiently large) that viscous effects become significant and dissipate turbulence energy as heat see figure 1. This process the continual creation of turbulence energy at large scales, transfer of energy to smaller and smaller eddies and the ultimate dissipation of turbulence energy by viscosity is called the turbulent energy cascade.

CLASSIFICATION OF TURBULENCE MODELS

Nowadays turbulent flows may be computed using several different approaches. Either by solving the Reynolds-averaged Navier-Stokes equations with suitable models for turbulent quantities or by computing them directly. The main approaches of turbulence modeling can be summarized by these models.

- Reynolds Average Navier-Stokes (RANS) Models.
- Large Eddy Simulations (LES)
- Direct Numerical Simulations (DNS)

Extension of modeling for certain CFD approach is illustrated in the following figure 2. It is clearly seen, that models computing fluctuation quantities resolve shorter length scales than models solving RANS equations. Hence they have the ability to provide better results. However they have a demand of much greater computer power than those models applying RANS methods.

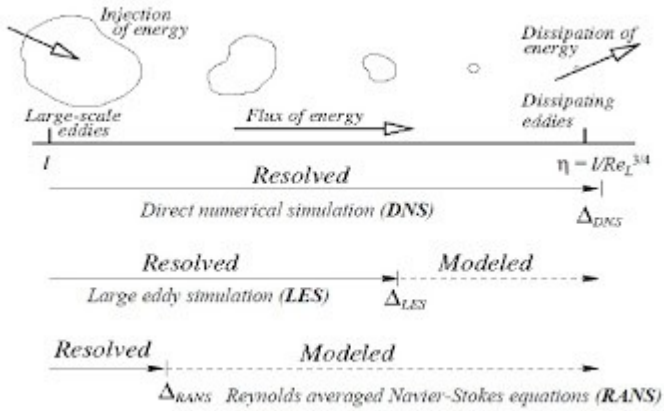

REYNOLDS AVERAGED NAVIER-STOKES (RANS) MODELS

The following section deals with the concept of Reynolds decomposition or Reynolds averaging. Any property (whether a vector or a scalar) can be written as the sum of an average and a fluctuation. This decomposition will yield a set of equations governing the average flow field. The new equations will be exact for an average flow field not for the exact turbulent flow field. By an average flow field we mean that
any property becomes constant over time. The result of using the Reynolds decomposition in the NS equations is called the RANS or Reynolds Averaged Navier Stokes Equations. Upon substitution of the Reynolds decomposition (for each variable, we substitute the corresponding decomposition) we
obtain the following RANS equations.

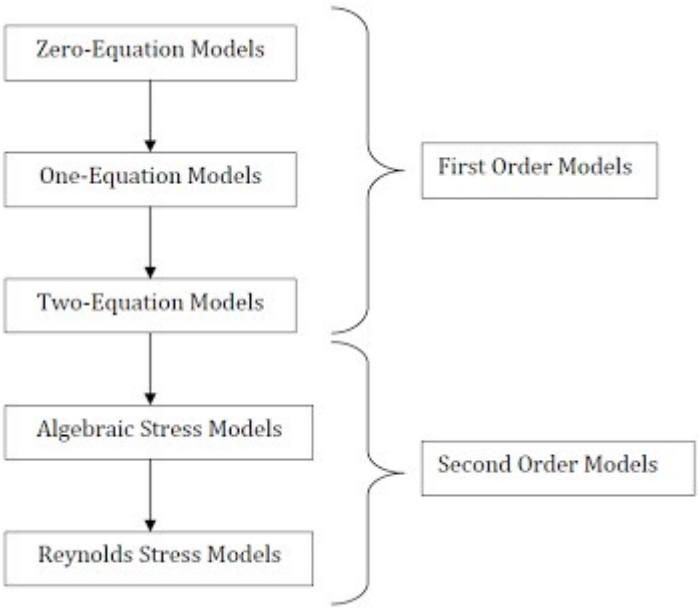

LARGE EDDY SIMULATION

Large eddy simulation (LES) is a popular technique for simulating turbulent flows. An implication of Kolmogorov's (1941) theory of self similarity is that the large eddies of the flow are dependant on the geometry while the smaller scales are more universal. This feature allows one to explicitly solve for the large eddies in a calculation and implicitly account for the small eddies by using a subgrid-scale model (SGS model).

Mathematically, one may think of separating the velocity field into a resolved and sub-grid part. The resolved part of the field represents the "large-scales"eddies, while the subgrid part of the velocity represents the "small-scales"whose effect on the resolved field is included through the subgrid-scale model. Formally, one may think of filtering as the convolution of a function with a filtering kernel G.

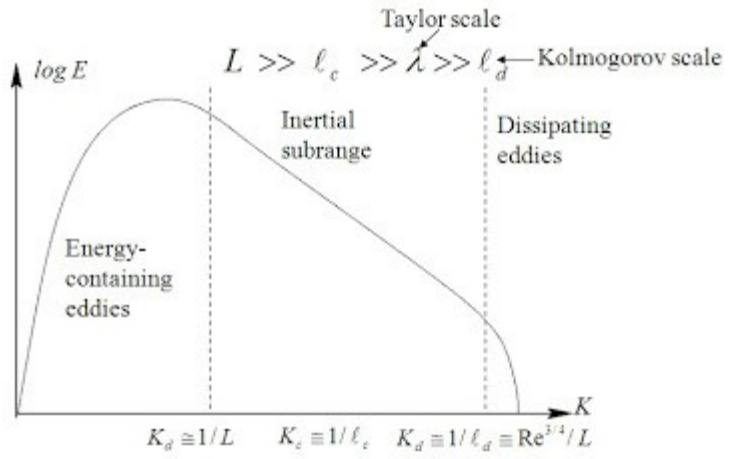

Energy cascade of Kolmogorov spectrum

From the figure.4 it is visible that the energy cascade of LES turbulence modeling using Kolmogorov
spectrum. Energy spectrum for LES, means that we have to consider the energy of large eddies plus the energy of subgrid scale. To find the energy for subgrid scale we have to derive it from Kolmogorov hypothesis, which means that for eddies much smaller than the energy containing eddies and much larger that dissipative eddies (of the order of Kolmogorov scales), turbulence is controlled solely by the dissipation rate and the size of the eddy (k), where k is the wave number and equals 1/L (L=size of eddies).

DIRECT NUMERICAL SIMULATION

A direct numerical simulation (DNS) is a simulation in computational fluid dynamics in which the Navier-Stokes equations are numerically solved without any turbulence model. This means that the whole range of spatial and temporal scales of the turbulence must be resolved. All the spatial scales of the turbulence must be resolved in the computational mesh, from the smallest dissipative scales (Kolmogorov scales), up to the integral scale L, associated with the motions containing most of the kinetic energy.

The computational cost of DNS is very high, even at low Reynolds numbers. For the Reynolds numbers encountered in most industrial applications, the computational resources required by a DNS would exceed the capacity of the most powerful computer currently available. However, direct numerical simulation is a useful tool in fundamental research in turbulence. Using DNS it is possible to perform “numerical experiments”, and extract from them information difficult or impossible to obtain in the laboratory, allowing a better understanding of the physics of turbulence. Also, direct numerical simulations are useful in the development of turbulence models for practical applications, such as sub-grid scale models for Large eddy simulation (LES) and models for methods that solve the Reynolds-averaged Navier-Stokes equations (RANS).

This is done by means of "*a priori*" tests, in which the input data for the model is taken from a DNS simulation, or by "a posteriori" tests, in which the results produced by the model are compared with those obtained by DNS.

DETACHED EDDY SIMULATION

The difficulties associated with the use of the standard LES models, particularly in near-wall regions, has lead to the development of hybrid models that attempt to combine the best aspects of RANS and LES methodologies in a single solution strategy. An example of a hybrid technique is the detached-eddy simulation (DES) approach. This model attempts to treat near-wall regions in a RANS-like manner, and treat the rest of the flow in an LES-like manner. The model was originally formulated by replacing the distance function d in the Spalart-Allmaras (S-A) model with a modified distance function.

This modification of the S-A model, while very simple in nature, changes the interpretation of the model substantially. This modified distance function causes the model to behave as a RANS model in regions close to walls, and in a Smagorinsky-like manner away from the walls. This is usually justified with arguments that the scale-dependence of the model is made local rather than global, and that dimensional analysis backs up this claim.
The DES approach may be used with any turbulence model that has an appropriately defined turbulence length scale (distance in the S-A model) and is a sufficiently localized model. The Baldwin-Barth model, while very similar to the S-A model, is probably not a candidate for use with DES. The standard version of this model contains several van Driest-type damping functions that make the distance function more global in nature. Menter's SST model is a good candidate, and has been used by a number of researchers. Menter's SST model uses a turbulence length scale obtained from the model's equations and compares it with the grid length scale to switch between LES and RANS.

In practice, more programming is needed than simply changing the calculation of the length scale. Many implementations of the DES approach allow for regions to be explicitly designated as RANS or LES regions, overruling the distance function calculation. Also, many implementations use different differencing in RANS regions (e.g. upwinded differences) and LES regions (e.g. central differences).

BOUNDARY LAYER

A boundary layer is a thin layer of viscous fluid close to the solid surface of a wall in contact with a moving stream in which (within its thickness δ) the flow velocity varies from zero at the wall (where the flow “sticks” to the wall because of its viscosity) up to U_e at the boundary, which approximately (within 1% error) corresponds to the free stream velocity (see Figure 1). Strictly speaking, the value of δ is an arbitrary value because the friction force, depending on the molecular interaction between fluid and the solid body, decreases with the distance from the wall and becomes equal to zero at infinity.

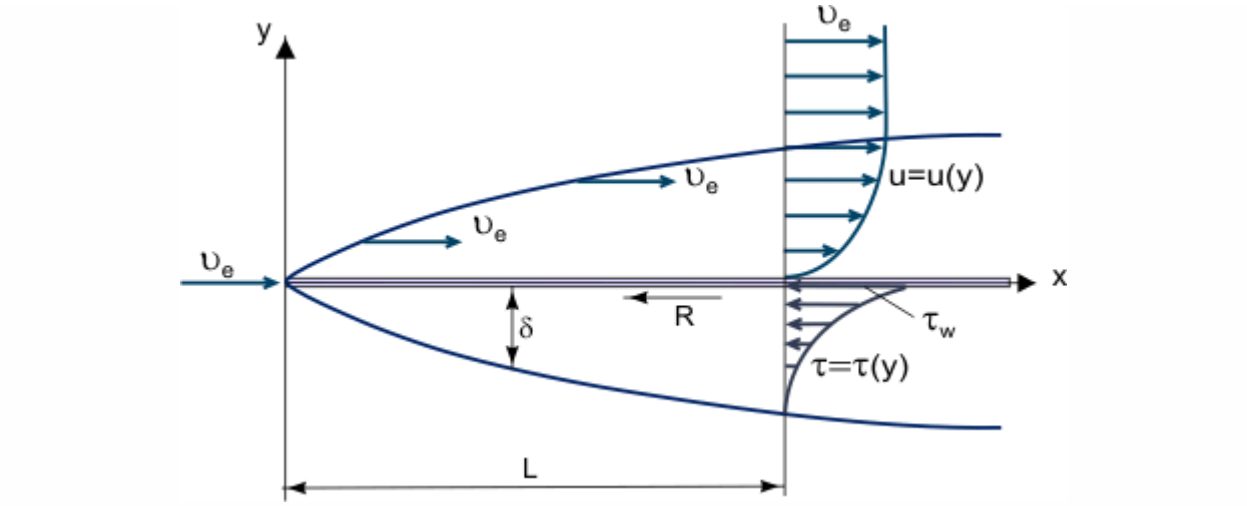

Figure1.Growth of a boundary layer on a flat plate.

The fundamental concept of the boundary layer was suggested by L. Prandtl (1904), it defines the boundary layer as a layer of fluid developing in flows with very high Reynolds Numbers Re, that is with relatively low viscosity as compared with inertia forces. This is observed when bodies are exposed to high velocity air stream or when bodies are very large and the air stream velocity is moderate. In this case, in a relatively thin boundary layer, friction Shear Stress (viscous shearing force): $\tau = \eta[\partial u/\partial y]$ (where η is the dynamic viscosity; $u = u(y)$ – "profile" of the boundary layer longitudinal velocity component, see Figure 1) may be very large; in particular, at the wall where $u = 0$ and $\tau_w = \eta[\partial u/\partial y]_w$ although the viscosity itself may be rather small.

It is possible to ignore friction forces outside the boundary layer (as compared with inertia forces), and on the basis of Prandtl's concept, to consider two flow regions: the boundary layer where friction effects are large and the almost Inviscid Flow core. On the premises that the boundary layer is a very thin layer ($\delta << L$, where L is the characteristic linear dimension of the body over which the flow occurs or the channel containing the flow, its thickness decreasing with growth of Re, Figure 1), one can estimate the order of magnitude of the boundary layer thickness from the following relationship:

(1)

$$\delta / L = Re^{-0.5}$$

For example, when an airplane flies at U_e = 400 km/hr, the boundary layer thickness at the wing trailing edge with 1 meter chord (profile length) is $\delta = 0.015$ m. As was experimentally established, a laminar boundary layer develops at the inlet section of the body. Gradually, under the influence of some destabilizing factors, the boundary layer becomes unstable and transition of boundary layer to a **Turbulent Flow** regime takes place. Special experimental investigations have established the

existence of a transition region between the turbulent and laminar regions. In some cases (for example, at high turbulence level of the external flow), the boundary layer becomes turbulent immediately downstream of the stagnation point of the flow. Under some conditions, such as a severe pressure drop, an inverse phenomenon takes place in accelerating turbulent flows, namely flow relaminarization.

In spite of its relative thinness, the boundary layer is very important for initiating processes of dynamic interaction between the flow and the body. The boundary layer determines the aerodynamic drag and lift of the flying vehicle, or the energy loss for fluid flow in channels (in this case, a hydrodynamic boundary layer because there is also a thermal boundary layer which determines the thermodynamic interaction of Heat Transfer).

Computation of the boundary layer parameters is based on the solution of equations obtained from the *Navier–Stokes equations* for viscous fluid motion, which are first considerably simplified taking into account the thinness of the boundary layer.

The solution suggested by L. Prandtl is essentially the first term of power series expansion of the Navier–Stokes equation, the series expansion being performed for powers of dimensionless parameter (δ/L). The smaller parameter in this term is in zero power so that the boundary layer equation is the zero approximation in an Asymptotic Expansion (at large Re) of the boundary layer equation (asymptotic solution).

A transformation of the Navier–Stokes equation into the boundary layer equations can be demonstrated by deriving the Prandtl equation for laminar boundary layer in a two-dimensional incompressible flow without body forces.

In this case, the system of Navier–Stokes equations will be:

(2)

$$\begin{cases} \dfrac{\partial u}{\partial t} + u\dfrac{\partial u}{\partial x} + v\dfrac{\partial u}{\partial y} = -\dfrac{1}{\rho}\dfrac{\partial p}{\partial x} + \nu\left(\dfrac{\partial^2 u}{\partial x^2} + \dfrac{\partial^2 u}{\partial y^2}\right), \\ \dfrac{\partial v}{\partial t} + u\dfrac{\partial v}{\partial x} + v\dfrac{\partial v}{\partial y} = -\dfrac{1}{\rho}\dfrac{\partial p}{\partial y} + \nu\left(\dfrac{\partial^2 v}{\partial x^2} + \dfrac{\partial^2 v}{\partial y^2}\right), \\ \dfrac{\partial u}{\partial x} + \dfrac{\partial v}{\partial y} = 0. \end{cases}$$

After evaluating the order of magnitude of some terms of Eq. (2) and ignoring small terms the system of Prandtl equations for laminar boundary layer becomes:

(3)

$$\begin{cases} \dfrac{\partial u}{\partial t} + u\dfrac{\partial u}{\partial x} + v\dfrac{\partial u}{\partial y} = -\dfrac{1}{\rho}\dfrac{\partial p}{\partial x} + v\left(\dfrac{\partial^2 u}{\partial x^2} + \dfrac{\partial^2 u}{\partial y^2}\right), \\ \dfrac{\partial u}{\partial x} + \dfrac{\partial v}{\partial y} = 0, \end{cases}$$

in which x, y are longitudinal and lateral coordinates (Figure 1); v is the velocity component along "y" axis; p, pressure; t, time; and n the kinematic viscosity.

The boundary layer is thin and the velocity at its external edge U_e can be sufficiently and accurately determined as the velocity of an ideal (inviscid) fluid flow along the wall calculated up to the first approximation, without taking into account the reverse action of the boundary layer on the external flow. The longitudinal pressure gradient $[\partial p/\partial x] = [dp/dx]$ (at $p(y) = const$) in Eq. (3) can be depicted from the *Euler equation of motion of an ideal fluid*. From the above, Prandtl equations in their finite form will be written as:

(4)

$$\begin{cases} \dfrac{\partial u}{\partial t} + u\dfrac{\partial u}{\partial x} + v\dfrac{\partial u}{\partial y} = \dfrac{\partial U_e}{\partial t} + U_e\dfrac{\partial U_e}{\partial x} + v\dfrac{\partial^2 u}{\partial y^2}, \\ \dfrac{\partial u}{\partial x} + \dfrac{\partial v}{\partial y} = 0. \end{cases}$$

This is a system of parabolic, nonlinear partial differential equations of the second order which are solved with initial and boundary conditions

$$\text{at } t = 0,\ u = u(0, x, y);\ y = 0,\ u = 0,\ v = 0;$$

$$y = \delta,\ u(t, x, y) = U_e(t, x);\ x = x_0,\ u = u_0(t, y).$$

The system of equations (4) is written for actual values of velocity components u and v. To generalize the equations obtained for turbulent flow, the well-known relationship between actual, averaged and pulsating components of turbulent flows parameters should be used. For example, for velocity components there are relationships connecting actual u and v, average ū and $\bar{v}$ and pulsating u' and v' components:

$$u = \bar{u} + u' \text{ and } v = \bar{v} + v'.$$

After some rearrangements, it is possible to obtain another system of equations [Eq. (6)] from system (3), in particular for steady flow:

(6)

$$\begin{cases} \bar{u}\dfrac{\partial \bar{u}}{\partial x}+\bar{v}\dfrac{\partial \bar{u}}{\partial y}=-\dfrac{1}{\rho}\dfrac{\partial \bar{p}}{\partial x}+\nu\dfrac{\partial^2 \bar{u}}{\partial y^2}-\dfrac{1}{\rho}\dfrac{\partial(\overline{\rho u'v'})}{\partial y}, \\ \dfrac{\partial \bar{u}}{\partial x}+\dfrac{\partial \bar{v}}{\partial y}=0. \end{cases}$$

Using the following relation for friction shear stress in the boundary layer:

(7)

$$\tau=\eta\frac{\partial \bar{u}}{\partial y}+\rho(-\overline{u'v'})$$

and taking into account that in the laminar boundary layer u = u' and $\rho\left(\overline{u',v'}\right)=0,$ it is possible to rewrite the Prandtl equations in a form valid for both laminar and turbulent flows:

(8)

$$\begin{cases} \bar{u}\dfrac{\partial \bar{u}}{\partial x}+\bar{v}\dfrac{\partial \bar{u}}{\partial y}=-\dfrac{1}{\rho}\dfrac{\partial \bar{p}}{\partial x}+\dfrac{1}{\rho}\dfrac{\partial \tau}{\partial y}, \\ \dfrac{\partial \bar{u}}{\partial x}+\dfrac{\partial \bar{v}}{\partial y}=0. \end{cases}$$

The simplest solutions have been obtained for a laminar boundary layer on a thin flat plate in a two-dimensional, parallel flow of incompressible fluid. In this case, the estimation of the order of magnitude of the equations terms: x ~ L, y ~ δ, δ ~ $\sqrt{\nu L/U_e},$ allows combining variables x and y in one relation

(9)

$$\xi=y\sqrt{u_e/(4\nu x)}$$

and to reduce the solution of Eq. (8) (at dp/dx = 0) to determining the dependencies of u and v upon the new parameter ξ. On the other hand, using well-known relations between velocity components u, v and stream function ψ

$$u=\partial\psi/\partial y,\quad v=-\partial\psi/\partial x$$

it is possible to obtain one ordinary nonlinear differential equation of the third order, instead of the system of partial differential equations (8)

(10)

$$2f'''(\xi)+f(\xi)f''(\xi)=0.$$

Here, f(ξ) is the unknown function of ξ variable: f = $f = \psi/\sqrt{u_e \nu x}.$

The first numerical solution of Eq. (10) was obtained by Blasius (1908) under boundary conditions corresponding to physical conditions of the boundary layer at y = 0: u = 0, v = 0; at y → ∞; u → U_e (Blasius boundary layer).

Figure 2 compares the results of *Blasius solution* (solid line) with experimental data. Using these data, it is possible to evaluate the viscous boundary layer thickness. At $\xi \simeq 2.5$, ($u/U_e \simeq 0.99$) (Figure 2); consequently from Eq. (9) we obtain: $\delta = 5\sqrt{vx/U_e}$.

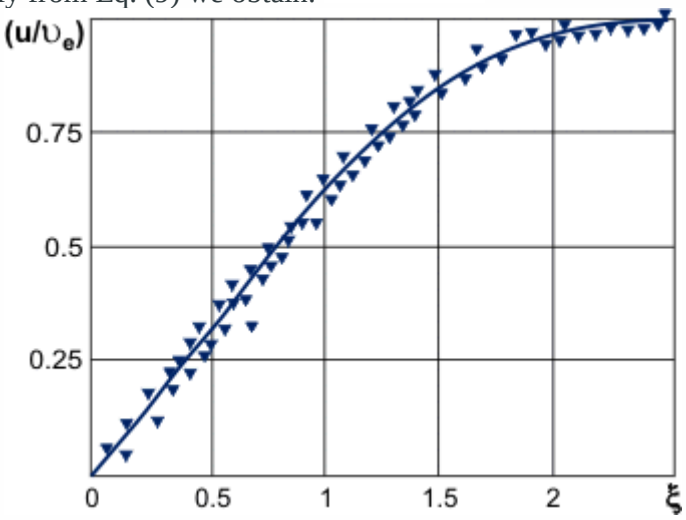

Figure2.

From the Blasius numerical calculations of the value of the second derivative of f(ξ) function at the wall friction shear stress, the relationship in this case is:

(11)

$$\tau_w = \eta[\partial u/\partial y]_{y=0} = \eta\frac{U_e}{4}\sqrt{U_e/(\eta x)}\, f''(\xi)_{y=0} \quad \text{or}$$

$$\tau_w = 0.664\rho(U_e^2/2)\sqrt{v/(U_e x)}.$$

Friction force R, acting on both sides of the plate of L length (Figure 1), is also determined from Eq. (11):

$$R = 2\int_0^L \tau_w\, dz = 0.664\sqrt{\rho\eta U_e^3 L},$$

as in the friction coefficient for flat plates:

$$\xi = R[(\rho U_e^2/2)L]^{-1} = 1.328\sqrt{v/(U_e L)}.$$

Despite the fact that Prandtl equations are much simpler than Navier–Stokes equations, their solutions were obtained for a limited number of problems. For many practical problems, it is not

necessary to determine velocity profiles in the boundary layer, only thickness and shear stress. This kind of information may be obtained by solving the integral momentum equation

(12)

$$\frac{d}{dx}\left[\int_0^\delta \rho u^2\, dy\right] - U_e \frac{d}{dx}\left[\int_0^\delta \rho u\, dy\right] = -\tau_w - \delta\frac{dp}{dx}.$$

The integral relationship (12) is valid both for the laminar and turbulent boundary layer.

Functions which were not known *a priori* but which characterize distribution of fluid parameters across the layer thickness δ are under the integral in Eq. (12). And the error of calculating the integral is less than the error in the approximately assumed integrand function ρu = ρu(y). These create conditions for developing approximate methods of calculating boundary layer parameters which are less time-consuming than the exact methods of integrating Prandtl equations. The fundamental concept was first suggested by T. von Karman, who introduced such arbitrary layer thickness δ*

(13)

$$\delta^* = \int_0^\delta \left[1 - \frac{u}{U_e}\right] dy$$

and momentum displacement thickness δ**

(14)

$$\delta^{**} = \int_0^\delta \frac{u}{U_e}\left[1 - \frac{u}{U_e}\right] dy.$$

thus, we can transform Eq. (12) for two-dimensional boundary layer of incompressible fluid to:

(15)

$$\frac{d}{dx}(\delta^{**}) + \frac{U_e'}{U_e}(\delta^* + 2\delta^{**}) = \frac{\tau_w}{\rho U_e^2}.$$

There are three unknown functions in Eq. (15), namely, δ* = δ*(x), δ** = δ**(x) and $\tau_w = \tau_w(x)$ [functions of $U_e(x)$ and correspondingly $U_e'(x)$, which are known from computations of flow in the inviscid flow core].

The solution of an ordinary differential equation like Eq. (15) usually requires assumption (or representation) of velocity distribution (velocity profile) across the boundary layer thickness as the function of some characteristic parameters (form-parameters), and it also requires the use of empirical data about the relationship between *friction coefficient* $C_f = 2\tau_w/(\rho U^2_e)$ and the arbitrary thickness of the boundary layer (friction law).

Some definite physical explanations can be given as far as the values of δ* and δ** are concerned. The integrand function in Eq. (13) contains after rearrangement, a term (U_e – u) which characterizes the velocity decrease. The integral in Eq. (14) can thus be considered as a measure of decreasing the flow rate across the boundary layer, as compared with the perfect fluid flow at the velocity U_e. On the other hand, the value of δ* can be considered as the measure of deviation along a normal to the wall (along "y" axis) of the external flow stream line under the influence of friction forces. From this consideration of the integral structure of Eq. (14), it is possible to conclude that δ** characterizes momentum decrease in the boundary layer under the influence of friction.

The following relations are valid:

$$\delta > \delta^* > \delta^{**} \text{ and } H = (\delta^* / \delta^{**}) > 1,$$

where H is the form-parameter of the boundary layer velocity profile. For example, for linear distribution u = ky,

$$\delta^* = (1/2)\delta,\ \delta^{**} = (1/6)\delta,\ H = 3.0.$$

At present, so-called semi-empirical theories are widely used for predicting turbulent boundary layer parameters. In this case, it is assumed that total friction stress τ in a turbulent boundary layer is a sum

(16)

$$\tau = \eta \frac{\partial \bar{u}}{\partial y} + \tau_T.$$

Here, τ_T is additional (turbulent or Reynolds) friction stress, in particular, in an incompressible flow $\tau_T = -\rho\left(\overline{u'v'}\right)$, see Eq. (7).

This representation is directly connected with the system of equations of motion in the boundary layer (6). In the compressible boundary layer, density pulsations can be considered to be the result of temperature pulsations

(17)

$$\tau_T = -\rho(\overline{u'v'})(1 - \beta),$$

where β = (1/T) is the volumetric expansion coefficient.

Additional semi-empirical hypotheses about turbulent momentum transfer are used for determining τ_T. For example,

$$\tau_T = \eta_T \frac{\partial \bar{u}}{\partial y},$$

where η_T is the dynamic coefficient of turbulent viscosity introduced by J. Boussinesq in 1877.

On the basis of the concept of similarity of molecular and turbulent exchange (*similarity theory*) Prandtl introduced the *mixing length (die Mischungsweg) hypothesis*. The mixing length 1 is the path a finite fluid volume ("mole") passes from one layer of average motion to another without changing its momentum. In accordance with this condition, he derived an equation which proved to be fundamental for the boundary layer theory:

(18)

$$\tau_t = \eta_T \frac{\partial \bar{u}}{\partial y} = \rho l^2 \left|\frac{\partial \bar{u}}{\partial y}\right| \frac{\partial \bar{u}}{\partial y}.$$

For turbulent region of the near wall flow boundary layer, L. Prandtl considered the length 1 proportional to y

(19)

$$l = \kappa y,$$

where κ is an empirical constant.

Close to the wall, where $\eta_T << \eta$, viscous molecular friction [the first term in Eq. (15)] is a determining factor. The thickness of this part of the boundary layer δ_1, which is known as laminar or viscous sublayer, is $= 0.01\delta$. Outside the sublayer, the value of η_T increases, reaching several orders of magnitude larger than η. Correspondingly, in this zone of the boundary layer known as the turbulent core $\tau_T > {}_0 = \eta[\partial\bar{u}/\partial y]$. Sometimes the turbulent core is subdivided into the buffer zone, where the laminar and turbulent friction are the comparable value, and the developed zone, where $\tau_T >> \tau_0$. For this region, after integrating Eq. (18) and taking into account Eq. (19), it is possible to derive an expression for *logarithmic velocity profile*:

(20)

$$u = \frac{1}{\kappa}\sqrt{\frac{\tau_w}{\rho}} \ln y + C.$$

If dimensionless (or universal) coordinates are used.

$$u^+ = u/v^* \text{ and } y^+ = v^* y/v,$$

where $v^* = \sqrt{(\tau_w/\rho)}$ is the so-called dynamic velocity (or Friction Velocity), Eq. (20) can be rewritten in the following form:

(21)

$$u^+ = \frac{1}{\kappa} \ln y^+ + B.$$

Velocity distribution representation in universal coordinates and mathematical models for turbulent viscosity coefficient are dealt with in greater detail in the section of Turbulent Flow.

One of the current versions of the semi-empirical theory of turbulent boundary layer developed by S. S. Kutateladze and A. I. Leontiev is based on the so-called asymptotic theory of turbulent boundary layers at $Re \rightarrow \infty$ where the thickness of laminar (viscous) sublayer δ_1 decreases at a higher rate than δ as a result of which $(\delta_1/\delta) \rightarrow 0$.

Under these conditions, a turbulent boundary layer with "vanishing viscosity" is developing. In this layer, $\eta \rightarrow 0$ but is not equal to zero and in this respect, the layer differs from perfect fluid flow. The concept of relative friction law, introduced by S. S. Kutateladze and A. I. Leontiev (1990), indicates

(22)

$$\Psi = (C_f / C_{f0}) \text{ at } Re^{**} = \text{idem}.$$

The law is defined as the ratio of friction coefficient C_f for the condition under consideration to the value of C_{f0} for "standard" conditions on a flat, impermeable plate flown around by incompressible, isothermal flow, both coefficients being obtained for $Re^{**} = U_e\delta^{**}/\nu$. It is shown that at $Re \rightarrow \infty$; $\eta \rightarrow 0$; and $C_f \rightarrow 0$, the relative variation of the friction coefficient under the influence of such disturbing factors as pressure gradient, compressibility, nonisothermicity, *injection (suction)* through a porous wall etc., has a finite value.

The equations derived for calculating the value of Ψ have one important characteristic which makes Ψ independent of empirical constants of turbulence. In accordance with the fundamental concept of the integral "approach", the integral momentum equation is transformed into:

(23)

$$\frac{d}{dx}(Re^{**}) + (1+H)\frac{Re^{**}}{U_e}U_e' = Re_L\frac{C_{f0}}{2}[\psi + b].$$

Here, $\bar{x} = x/L$, $Re_L = U_eL/\nu$, $b = (2/C_{f0})(\rho_wU_w)/(\rho_eU_e)$ are the permeability parameters for the case of injecting a gas at density ρ_w through a permeable wall at the velocity of v_w. For determining the function $Re^{**} = Re^{**}(\bar{x})$, it is necessary to calculate the distribution $\Psi = \Psi(\bar{x})$. For this purpose, the principle of superposition of disturbing factors applies

(24)

$$\Psi = \Psi_M \cdot \Psi_T \cdot \Psi_B \cdot \Psi_P \ldots.$$

In Eq. 24, each multiplier represents the relative friction law, taking into account the effect of one of the factors, among them *compressibility* Ψ_M, temperature head Ψ_T, injection Ψ_B, pressure gradient Ψ_P and others.

The fundamental concepts of the boundary layer create conditions for explaining such phenomena as *flow separation*from the surface under the influence of the flow inertia, deceleration of viscous flow by the wall and adverse pressure gradient acting in the upstream direction $[\partial p/\partial x] = [dp/dx[>] 0$ or $[\partial u/x\partial] < 0$.

If pressure gradient is adverse on the surface location between sections '1–4' (see Figure 3), the velocity distribution u = u(x,y) in the boundary layer changes gradually; becoming "less full," decreasing the inclination in the fluid jets which are closer to the wall and possessing less amount of kinetic energy (see velocity profile shapes in Figure 3) which penetrate far downstream into the region of increased pressure. In some sections, for example section '4', fluid particles which are on the 'a-a' stream line (dotted line in Figure 3) — having completely exhausted their supply of kinetic energy become decelerated ($u_a = 0$).

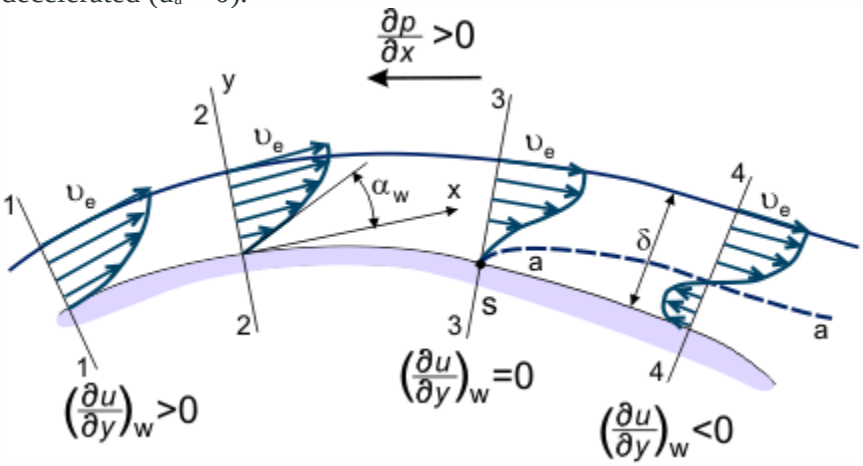

Figure3.Boundary layer in flow over a covered surface.

Static pressure and pressure gradient value do not vary across boundary layer thickness. Therefore, fluid particles which are closer to the wall than line 'a–a' and possessing still less amount of energy begin to move in the opposite direction under the influence of the pressure gradient in '4–4' section (see Figure 3). Thus, the relationship:

$$\tan \alpha_w = [\partial u / \partial y]_w < 0 .$$

In this way, at some locations of the surface, the velocity profile changes. This change is characterized by the alteration of the sign of the derivative $[\partial u/\partial y]_w$ from positive to negative (section 4). Of course, it is also possible to define the section where $[\partial u/\partial y]_w = 0$ .This is referred to

as the *boundary layer separation* section (correspondingly point ‘S’ on the surface of this section is the separation point). It is characterized by the development of a reverse flow zone — the flow around the body is no longer smooth, the boundary layer becomes considerably thicker and the external flow stream lines deviate from the surface of the body flown around. Downstream of the separation point, the static pressure distribution across the thickness of the layer is not steady and the static pressure distribution along the surface does not correspond to the pressure distribution in the external, inviscid flow.

The separation is followed by the development of reverse flow zones and swirls, in which the kinetic energy supplied from the external flow transforms into heat under the influence of friction forces. The flow separation, accompanied by energy dissipation in the reverse flow swirl zones, results in such undesirable effects as increases in the flying vehicles’ drag or hydraulic losses in channels.

On the other hand, separated flows are used in different devices for intensive mixing of fluid (for example, to improve mixing of fuel and air in combustion chambers of engines). When viscous fluids flow in channels with a variable cross-section (alternating pressure gradient), the separation zone may be local if the diffusor section is followed by the confusor section, where the separated flow will again reattach to the surface . When the flow separates from the trailing edge of the body (for example, from the wing trailing edge), the so-called *wake* is formed by “linking” boundary layers .